

Computational Reconstruction of the Probable Change of Form of the Corneal Lens and Maturation of Optics in the Post-ecdysial Development of the Schizochroal Eye of the Devonian Trilobite *Phacops rana milleri* Stewart 1927

GÁBOR HORVÁTH† AND EUAN N. K. CLARKSON‡§

† *Institute for Zoology, University of Regensburg, University Street 31, P.O.B. 101042, D-8400 Regensburg, Germany and Central Research Institute for Physics of the Hungarian Academy of Sciences, Biophysics Group, H-1525 Budapest, P.O.B. 49, Hungary and* ‡ *University of Edinburgh, Department of Geology and Geophysics, Grant Institute, West Mains Road, Edinburgh EH9 3JW, Scotland, U.K.*

(Received on 10 September 1991, Accepted on 9 July 1992)

Trilobites had to redevelop their corneal lenses after each moult, since the old lenses remained with the discarded exoskeleton. Earlier, Miller & Clarkson (1980) were able to reconstruct three main stages of the post-ecdysially developing lenses in the schizochroal compound eye of the Devonian trilobite *Phacops rana milleri* Stewart, 1927. In this present work it is shown that the conical, then saucer-like and later wave-shaped proximal profile of the lens in these developmental stages is consistent with a Huygensian correction for spherical aberration as postulated for the adult eyes of some other trilobites by Clarkson & Levi-Setti (1975).

The focal length of the developing lens is determined as a function of the lens thickness comparing and fitting the theoretically calculated Huygensian profiles to the experimentally reconstructed real lens surfaces. Using an empirical quadratic function fitted onto the variation of focal length versus lens thickness, a probable series of change of form of the developing lens in *Phacops rana milleri* is reconstructed computationally. On the basis of the geometric optical model presented, a further possible transitional stage between the shape of the last stage of the post-ecdysially developing lens and its mature form can be derived.

Using geometric optical formulae for thick lenses and paraxial approximation, many features of image construction have been estimated for the post-ecdysial development of the eye. The actual position of the retina below the lens, and whether this changed during post-ecdysial development, remains unknown from fossilized material. It has been possible, however, to calculate object position and magnification at all stages of post-ecdysial development, from the shape and thickness of the lens.

Likewise, the positions of the retina for which *Phacops rana milleri* could take advantage of its spherically corrected Huygensian lenses are established here. It is probable that the retina was fixed or moved little during the post-ecdysial stages. If so the eye was myopic in the earliest developmental stage, but thereafter could see sharply at a distance of a few millimetres to a few centimetres from the visual surface. Depending on the receptor separation in the retina, the depth of focus estimated was several centimetres so that the depth in object space could reach one decimetre, over which the image was in focus in the developing eye.

† Author to whom correspondence should be addressed.

1. Introduction

As with modern arthropods, the extinct trilobites shed their exoskeletons periodically to accommodate changes in size and shape produced by their growth. The majority of trilobite remains represent cast-off shields or exuviae. Ecdysis itself is a period of considerable physiological stress, accounting for a large percentage of mortality.

Specimens of the Devonian trilobite *Phacops rana milleri* Stewart 1927 from the Middle Devonian Silica Shale of Ohio (Eldredge, 1972) are sometimes preserved in the early stages of the post-ecdysial cycle; such individuals represent remains of animals that died before their post-ecdysial development was complete. Such specimens as these allowed Miller & Clarkson (1980) to determine how much cuticular carbonate was removed and renewed during moulting, how the layers of cuticle were built up post-ecdysially and how specialized cuticular organs, especially the schizochroal compound eyes, were reconstructed immediately after exuviation. Trilobites had to redevelop their corneal lenses after each moult, since the old lenses remained with the discarded exoskeleton.

In the developing eyes of individuals that died in the early stages of the post-ecdysial cycle, each of the lenses had initially the form of a small, simple calcite cone hanging from the lower surface of the cornea. In later stages this post-ecdysial lens spread to the full width of the lens capsule, losing its conical form, taking on proximally a saucer-like and, later, a wavy Huygensian shape, and eventually acquiring its mature form in which there was a central core and, proximally, a thin intralensar bowl.

The significance of lens doublets in trilobite eyes was first established by Levi-Setti (Clarkson & Levi-Setti, 1975). It was shown that in the eye of the Ordovician trilobite *Crozonaspis struvei* Henry 1968 the lens consists of two components, an upper lens unit, separated by a wavy lower surface from a basal intralensar bowl. The shape of the upper lens unit is effectively identical to that of an ideal aplanatic thick lens, as designed by Huygens (1690), and the later addition of the intralensar bowl during development makes a lens-doublet system. Experimental models of such a lens were tested and found to be highly efficient. A different kind of lens-doublet system is found in *Dalmanitina socialis*, where the surface separating the upper lens unit from the intralensar bowl conforms to DesCartes' (1637) alternative model. Miller & Clarkson (1980) suggested that the lenses of *Phacops rana milleri* might function in the same general way, but in this trilobite the lens-system is somewhat unusual since there is an additional central core, and the intralensar bowl becomes very thin or absent centrally.

It seems pertinent to consider whether the conical shape of the immediately post-ecdysial lens and the later saucer-like and wavy form was a functional adaptation or merely a record of the only way in which the lens could grow. The analysis of the optics of the different developmental stages was beyond the scope of the earlier anatomical work by Miller & Clarkson (1980) on the post-ecdysial development of the cuticle and the eye of the trilobite *Phacops rana milleri*. Recently, one of the authors of this paper (Horváth, 1989a, b) developed a general geometric optical

method for fast computer calculation of optimal refractive interfaces. This has been used in analysis of the schizochroal eyes of trilobites (Clarkson, 1979) corrected for spherical aberration (Horváth, 1989a), also in the water bug *Notonecta* (Schwind, 1980, 1985), the corneal lenses of which have a very similar function and structure (Horváth, 1989b; Horváth & Greguss, 1989a, b) and likewise in the mirror-lens eye of the scallop *Pecten* (Land, 1965, 1968), the visual system of which corresponds to the Schmidt astronomical telescope (Horváth & Varjú, 1993). This computer method makes it possible to study computationally the optics of the different developmental stages of the post-ecdysial lens in the trilobite *Phacops rana milleri* and to answer the following important paleobio-optical questions.

(a) Whether the conical and, later, saucer-like proximal surface of the lens in the early post-ecdysial eye of *Phacops rana milleri* has an optimized shape corrected for spherical aberration, as has the wave-shaped Huygensian lens profile in the later stage of development.

Whereas earlier Miller & Clarkson (1980) had considered the proximal lens profile to be Huygensian only in the latest post-ecdysial state of development immediately preceding the mature form with core and intralensar bowl, it is the case that conical and saucer-like shapes can also be Huygensian. If question (a) is answered positively then the following question arises.

(b) To what extent did the distance of the retina from the corneal surface have to change during post-ecdysial development, in order that *Phacops rana milleri* might take advantage of such an aplanatic dioptric element? Clearly, the enhanced image quality and light-collecting efficiency given by a spherically corrected Huygensian lens will only operate where the retinal surface falls at an appropriate distance from the corneal lens.

Although a substantial amount of fossil material was available to Miller & Clarkson (1980), only a few post-ecdysial stages were found amongst it. The developmental series which they reconstructed remains incomplete, and several important stages are still unknown. In particular, the critical transition from the Huygensian post-ecdysial lens (Fig. 1) to the mature stage (Figs 2 and 3) with the bowl and core differentiated has not been documented. Thus two further questions arise.

(c) Is it possible to reconstruct, approximately, how the shape of the post-ecdysially developing lens in the eye of *Phacops rana milleri* changed on the basis of the few stages of development known from anatomical studies?

(d) How did the lens achieve the transition from the shape of the last known stage of the post-ecdysially developing lens to its mature form?

In spite of the great body of information accumulated on the visual system of trilobites in the last 25 years (Clarkson, 1966a, b, 1967, 1968, 1969, 1971, 1973, 1975, 1979; Towe, 1973; Campbell, 1975; Stockton & Cowen, 1976; Feist & Clarkson, 1989; Fordyce & Cronin, 1989; Horváth, 1989a; Zhang & Clarkson, 1990), these questions have not yet been answered. In this present work, after a brief review of the mature schizochroal compound eye and its lens structure in the trilobite *Phacops rana milleri* and that of its post-ecdysially developing lenses, we investigate theoretically the Huygensian profile of a thick lens corrected for spherical aberration as a function of the lens thickness and the focal length, and furthermore the optical

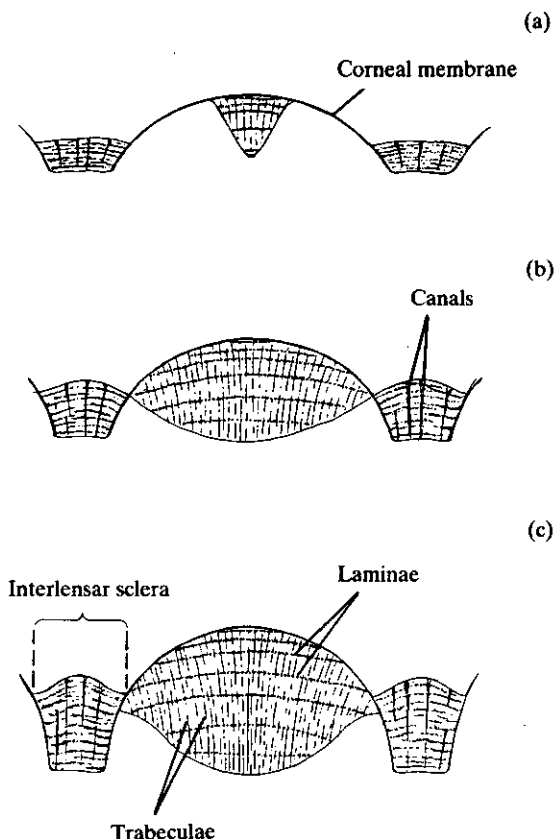


FIG. 1. Three stages of the post-ecdysial development of the lens in *Phacops rana milleri* as reconstructed by Miller & Clarkson (1980). (a) Initial small lens with conical, slightly incurved proximal surface; (b) thin biconvex lens with saucer-like proximal surface; (c) thick lens with wavy proximal profile, before the differentiation of the core and addition of the intralensar bowl. The values of the lens thickness a of these developmental stages can be found in Table 1.

features of image construction of the developing lens in order to answer the above paleobio-optical questions.

2. The Mature Eye and its Lens Structure in *Phacops rana milleri*

In the adult *Phacops rana milleri* the eyes are large relative to the head of the trilobite. Each eye has about 90 lenses or less, set upon a curving visual surface in the standard pattern of hexagonal close packing, normal in schizochroal-eyed phacopid trilobites. In the adult there are some 17 dorso-ventral files with a maximum of seven lenses, intersecting with diagonal rows: the lenses increase in size slightly from the top to the bottom of the visual surface. The lenses are separated from one another by "interlensar sclera", a material identical with the rest of the exoskeleton. The maximum size of the lenses is about 0.5 mm. The adult eye subtends a visual field

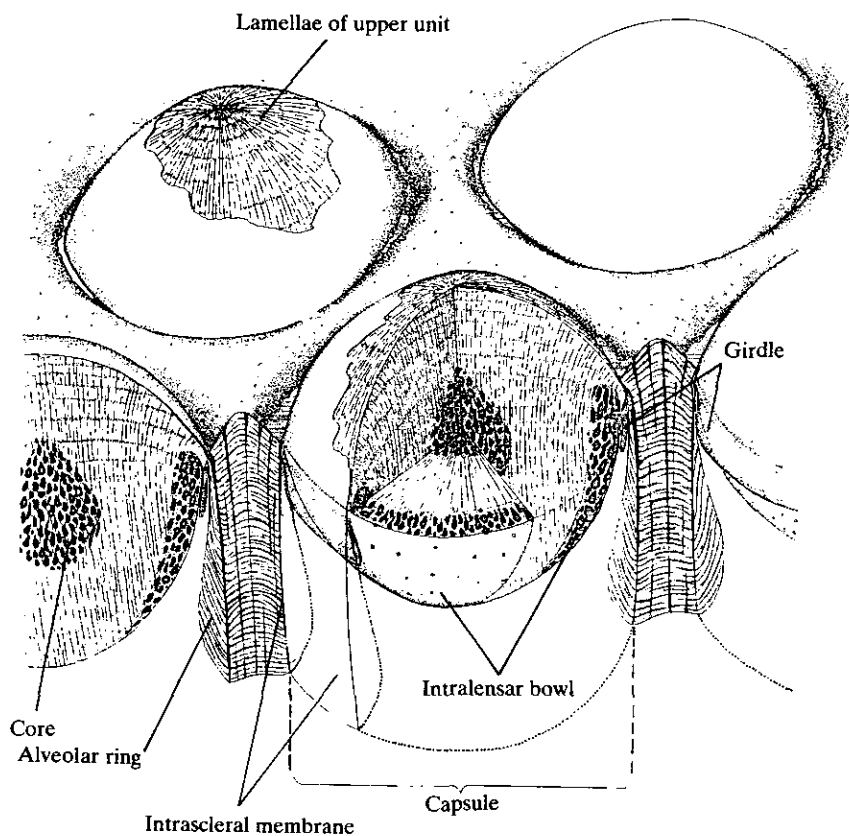


FIG. 2. Diagrammatic representation of the mature schizochroal compound eye of the Devonian trilobite *Phacops rana milleri* Stewart 1927, with lenses dissected to show internal structure. Details of corneal structure have been omitted for clarity (Miller & Clarkson, 1980).

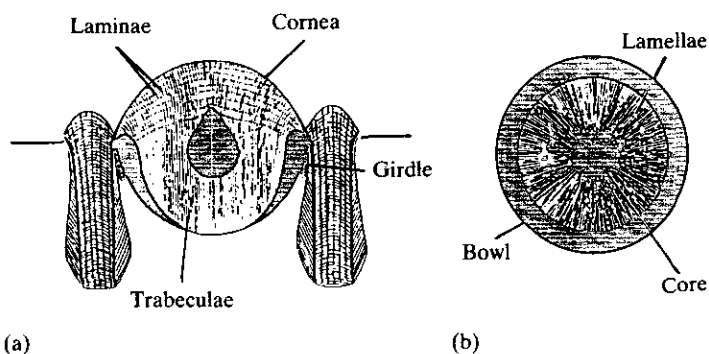


FIG. 3. Vertical (a) and horizontal (b) section of a lens in the eye of *Phacops rana milleri* (Clarkson, 1979).

of some 30° above the horizontal (i.e. the trilobite's equatorial plane), and the visual fields of the two eyes meet at front and rear.

Each of the lenses is almost spherical and is set at the top of an alveolus, a cylindrical cavity walled by interlensar sclera [Figs 2, 3 and 4(f)]. Through this passes an "intrasceral membrane" continuous with the thin cornea, which covers the lens. It is probable that this membrane was extended below the lens to form a capsule floored by a flat retina of photosensitive cells. These were presumably linked to an optical ganglion and thence to the animal's central nervous system, though there is no direct evidence of what the photosensitive parts of the eye were actually like.

The adult lens is a single crystal of calcite, but various components were differentiated within it. The main part (upper unit) of the lens is constructed of radial lamellae. These are made of calcite needles (trabeculae), which are generally parallel with the lens axis, but which are turned outwards towards the top so as to make an angle of some 70° towards its periphery.

In the centre of the lens is a pear-shaped core of dense ferroan calcite, which is very similar to the structure of the intralensar bowl in the proximal part of the lens. Whereas such a bowl is constant in phacopid trilobites (except where diagenetically altered) the bowl of *Phacops rana milleri* is rather unusual since it thins out, almost vanishing below the core. Otherwise the bowl is a pronounced, and constant, structure rising high up the sides of the lens, and with a thick and rounded upper rim. Some further, minor details of the structure of the lens are given in Miller & Clarkson (1980).

3. Post-ecdysial Development of the Lens in *Phacops rana milleri*

With reference to the anatomical reconstructions made by Miller & Clarkson (1980), the development of the lens in *Phacops rana milleri* from a very early post-ecdysial stage to maturity is as follows [Figs 1 and 4(a)–(f)].

(I) In the first stage of development, the cornea was still flexible, and where it was translucent in the investigated material the embryonic upper unit of the lens could be seen as a clear, small, dark circle, 150 µm across in the centre of the lens. The whole corneal surface was about 650 µm across and the lens hung suspended from the proximal surface of the cornea [Figs 1(a) and 4(a)–(c)]. At this stage the lens formed a steep-sided cone whose proximal point lay in approximately the same plane as the lower surface of the sclera. The proximal surface of the cone was slightly incurved and the tip truncated. This early stage in the development of the lens was constructed on a radial plan.

(II) The next stage in development is shown in Figs 1(b) and 4(d). Here the lens has grown right to the periphery of the cornea and has lost its conical form, becoming biconvex with the saucer-like proximal surface being less evidently curved than in stage (I). The lowermost part of the lens still lay in approximately the same plane as the proximal edge of the sclera.

(III) A little later, the lens has become thicker, as has the sclera, and the proximal surface of the lens has assumed a Huygensian form [Figs 1(c) and 4(e)]. There were curved laminations in the upper part of the lens.

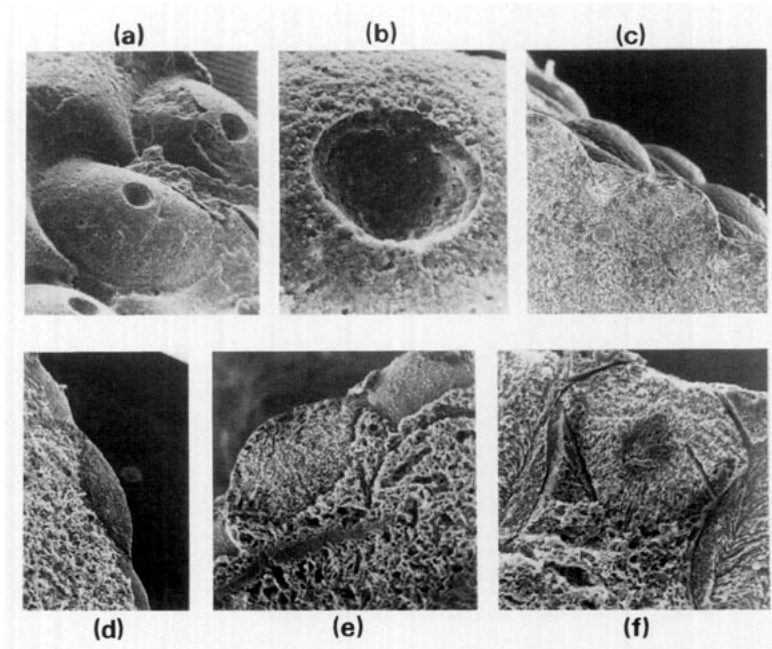


FIG. 4. Structure of the developing eye in *Phacops rana milleri*. (a) Surface of the eye of the earliest post-ecdysial stage, after an etching process which has dissolved out the small conical lenses; $\times 60$ [cf. Fig. 1(a)]. (b) Detail of a single etched conical lens; $\times 315$. (c) Vertical section of lenses at the earliest post-ecdysial stage, showing thin cuticle and conical form of lenses; $\times 32$. (d) Vertical section through part of eye, a later post-ecdysial stage where the lens is now of biconvex form with saucer-like proximal surface; $\times 32$ [cf. Fig. 1(b)]. (e) Vertical section through lens at a still later stage, equivalent to Fig. 1(c); $\times 45$. (f) Vertical, etched section through mature lens, showing the intralensar bowl, core and etched-out cleavage planes in the calcite; $\times 60$ [cf. Figs 2 and 3(a)].

(IV) This state of development was an intermediate transition between stage (III) and the following mature stage (V). Details are not known, but the proximal growth of the lens must have stopped peripherally and continued centrally in order that the bowl-like proximal surface of the upper lens unit would take shape subsequently.

(V) The mature lens had a properly developed intralensar bowl, and a central core [Figs 2, 3 and 4(f)]. It was much thicker than in stage (III) but, for the first time, the sclera has thickened greatly so that its proximal surface lay well below the base of the lens. At all previous stages of development the lens capsule was bounded internally by the inner face of the corneal cylinder, but in the mature lens both the girdle and the alveolar ring have grown inside the cylinder and were clearly very late-stage developments. Though all these new developments happened quite rapidly, it is not possible to decide whether they took place in a particular sequence or developed more or less simultaneously.

The post-ecdysial development of the lens in *Phacops rana milleri* was thus a process involving several stages of growth. There was only little change in the curvature of the upper surface of the cornea, and new material was accreted exclusively on the lower part of the lens and on the inner wall of the lens capsule (Miller & Clarkson, 1980).

4. Calculation of the Huygensian Profile

Consider the optically homogeneous post-ecdysial singlet lens of refractive index $n_L = 1.66$ (calcite, along c -axis) in the eye of *Phacops rana milleri*, the distal and proximal surface of which is in contact with water of refractive index $n_w = 1.33$ and body fluid of index $n_B = 1.34$, respectively (Fig. 5). Functions $f(x)$ and $H(y)$ describe the vertical section of the distal and proximal surface of the lens in the system of co-ordinates of Fig. 5. The thickness of the lens is a and its radius of aperture r_a . In this section we determine the proximal Huygensian profile $H(y)$ which ensures that the lens is corrected for spherical aberration, that is, all the paraxially incident rays of light intersect the optical axis at the same focal point F after the refraction on the boundary surfaces of the lens. Focal point F is at a distance L from the proximal lens surface.

Using the Snell's law of refraction, on the basis of Fig. 5 the following can be written

$$n_w \sin \alpha = n_L \sin \beta, \quad (1)$$

$$n_L \sin \gamma = n_B \sin \delta, \quad (2)$$

$$\alpha - \beta = \gamma - \omega, \quad (3)$$

$$\delta = \omega + \varepsilon, \quad (4)$$

$$x = y + [a - H(y) + f(x)] \tan (\alpha - \beta), \quad (5)$$

$$y = [L + H(y)] \tan \varepsilon, \quad (6)$$

$$\tan \omega = H'(y) \equiv \frac{dH(y)}{dy}, \quad (7)$$

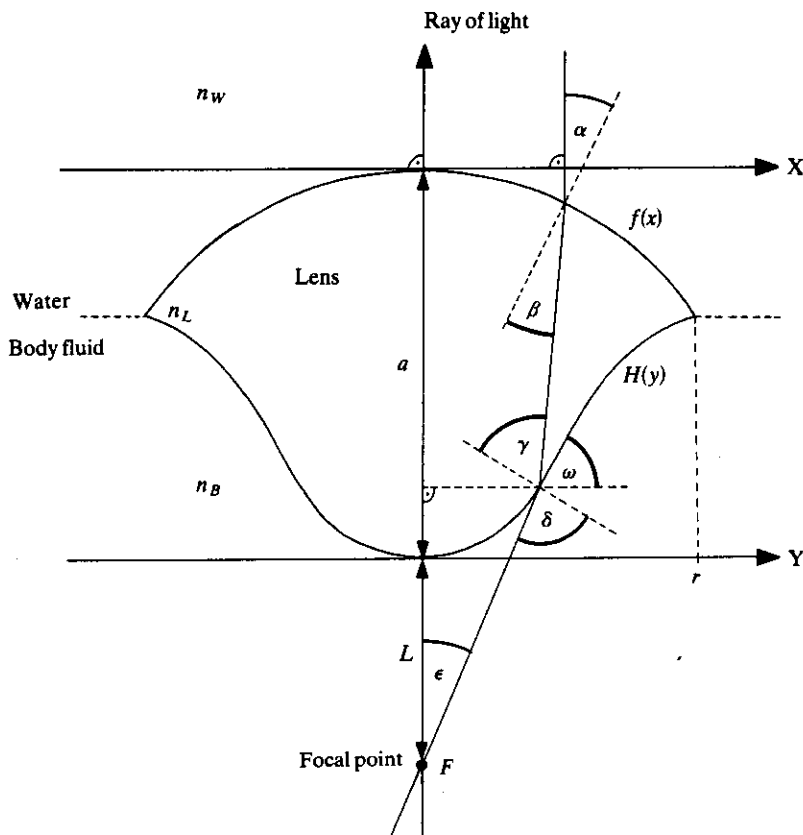


FIG. 5. Path of a paraxially incident ray of light in a thick lens of thickness a and refractive index $n_L = 1.66$ (calcite, along c -axis) contacting distally with water of refractive index $n_w = 1.33$ and proximally with body fluid of index $n_B = 1.34$. The ray intersects the optical axis at the focal point F after the refraction on the distal and proximal lens surfaces, the vertical sections of which are described by functions $f(x)$ and $H(y)$, respectively. If $H(y)$ is Huygensian the lens is corrected for spherical aberration, that is, it is aplanatic.

$$\tan \alpha = -f'(x) \equiv -\frac{df(x)}{dx}. \quad (8)$$

From (2-7) one can obtain

$$\sum_{i=0}^4 p_i [H'(y)]^i = 0 \quad (9)$$

with the parameters

$$\begin{aligned} p_0 &= k_1 k_4 + k_3 k_7, \\ p_1 &= p_3 = k_2(k_4 - k_7) + k_5(k_1 + k_3), \\ p_2 &= k_1(k_6 + k_7) + k_3(k_4 + k_8), \\ p_4 &= k_1 k_8 + k_3 k_6, \end{aligned} \quad (10)$$

where

$$\begin{aligned}k_1 &= (x-y)^2, & k_2 &= 2(x-y)[a-H(y)+f(x)], \\k_3 &= [a-H(y)+f(x)]^2, & k_4 &= -y^2(n_L^2-n_B^2)-n_L^2[L+H(y)]^2, \\k_5 &= 2n_B^2y[L+H(y)], & k_6 &= -(n_L^2-n_B^2)[L+H(y)]^2-n_L^2y^2, \\k_7 &= n_B^2y^2, & k_8 &= n_B^2[L+H(y)]^2.\end{aligned}\quad (11)$$

From (1), (5) and (8) the following can be obtained

$$y-x+[a-H(y)+f(x)]G(x)=0, \quad (12)$$

where

$$G(x) \equiv f'(x) \frac{n_w - [n_L^2 + (n_L^2 - n_w^2)f'(x)^2]^{1/2}}{[n_L^2 + (n_L^2 - n_w^2)f'(x)^2]^{1/2} + n_w f'(x)^2}. \quad (13)$$

From (12) it follows

$$y + \Delta y - (x + \Delta x) + [a - H(y + \Delta y) + f(x + \Delta x)]G(x + \Delta x) = 0, \quad (14)$$

from which

$$\Delta y = \frac{y - (x + \Delta x) + G(x + \Delta x)[a + f(x + \Delta x) - H(y)]}{G(x + \Delta x)H'(y) - 1}. \quad (15)$$

The initial conditions are

$$y(x=0) = H(y=0) = H'(y=0) = 0. \quad (16)$$

The value of $H(y + \Delta y)$ can be obtained from

$$H(y + \Delta y) = H(y) + H'(y)\Delta y. \quad (17)$$

After this one can determine the Huygensian profile $H(y)$ in the following way. When $y(x)$, $H(y)$, $H'(y)$ are already known for a given x one gets a step Δx (>0) and using $x + \Delta x$, $f(x + \Delta x)$, $G(x + \Delta x)$, $y(x)$, $H(y)$, $H'(y)$ calculates Δy from (15). Then using $H(y)$, $H'(y)$, Δy one calculates $H(y + \Delta y)$ on the basis of (17). Eventually using $y + \Delta y$, $H(y + \Delta y)$, $x + \Delta x$, $f(x + \Delta x)$, $G(x + \Delta x)$ one obtains $H'(y + \Delta y)$ solving (9). The algorithm of this numerical procedure can be seen in Fig. 6(a) with the initial conditions shown in Fig. 6(b).

5. The Huygensian Profile as a Function of Lens Thickness and Focal Length

The shape of the vertical section of the distal surface of the lens in the mature eye of *Phacops rana milleri* can be well approximated by the function

$$f(x) = d \sqrt{1 - \left(\frac{x_2}{r}\right)^2} - d \quad \text{with } d = 650 \mu\text{m}, r = 635 \mu\text{m} \quad (18)$$

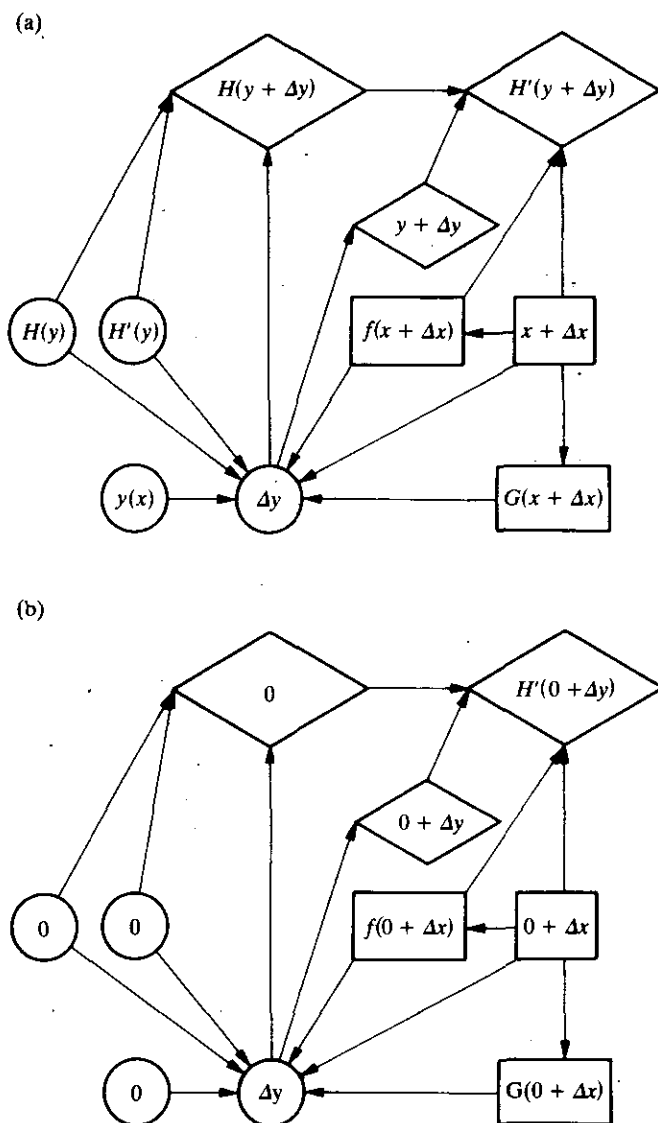


FIG. 6. (a) Algorithm of the numerical calculation of the proximal Huygensian profile $H(y)$; (b) initial conditions of the procedure.

on the basis of the anatomical reconstruction made by Miller & Clarkson (1980), where d is the height of the corneal surface and r is the lens radius. Since the curvature of the upper surface of the lens changed very little, and furthermore new material was accreted exclusively on the lower part of the lens and on the inner wall of the lens capsule during post-ecdysial development (Miller & Clarkson, 1980), the distal surface of the developing lens can also be approximated by function (18).

First consider the shape of the Huygensian profile $H(y)$ as a function of the focal length L for a given lens thickness a . Using the computer method presented in the previous section, the results are shown in Fig. 7 for the three different values of a of Fig. 1 (see Table 1). From the family of curves of Fig. 7 we can see that at a

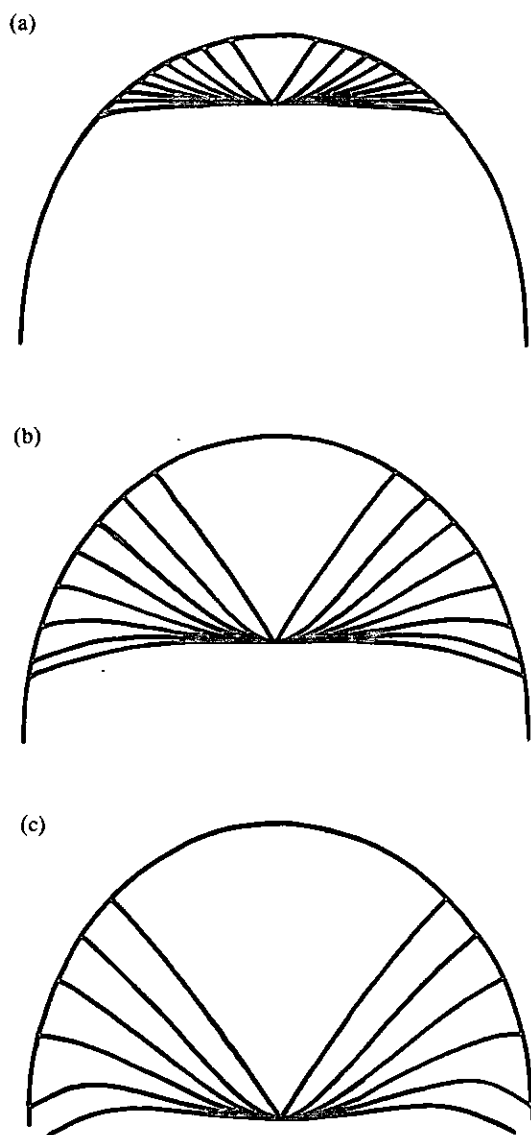


FIG. 7. Family of proximal Huygensian lens profiles calculated theoretically as a function of the focal length L and the lens thickness a , the numerical values of which are the same as those in Fig. 1. $L_i = L_0 + (i-1)\Delta L$, $i = 1, 2, \dots, N$; $L_0 = 10 \mu\text{m}$, $\Delta L = 300 \mu\text{m}$. (a) $a_1 = 150 \mu\text{m}$, $N = 9$; (b) $a_2 = 450 \mu\text{m}$, $N = 8$; (c) $a_3 = 650 \mu\text{m}$, $N = 6$.

TABLE 1

Values of the optical and geometrical parameters of the developing trilobite singlet lens

	Lens 1 Stage (I) of Fig. 1(a)	Lens 2 Stage (II) of Fig. 1(b)	Lens 3 Stage (III) of Fig. 1(c)
(a) a (μm)	$a_1 = 150$	$a_2 = 450$	$a_3 = 650$
(b) L (μm)	$L_1 = 50$	$L_2 = 950$	$L_3 = 850$
(c) q	$q_1 = -872.5 \mu\text{m}$	$q_2 = 7.2$	$q_3 = -0.007 \mu\text{m}^{-1}$
(d) r_p (μm)	-12.2	-405.6	-353.8
(e) g_{11}	-1.3712	0.7861	0.6458
(f) g_{12} ($10^{-3} \mu\text{m}^{-1}$)	25.512	1.207	1.248
(g) g_{21} (μm)	-90.36	-271.08	-391.57
(h) g_{22}	0.9519	0.8558	0.7917
(i) L' (μm)	52.5	1110	1073.6

(a) Numerical values of the lens thickness a in the three stages of post-ecdysial development of Fig. 1 reconstructed by Miller & Clarkson (1980) in *Phacops rana milleri*. (b) Numerical values of the focal length L of those theoretical Huygensian singlet lenses corrected for spherical aberration which fit best with the real ones of Fig. 1. (c) Numerical value of the parameters (q_1, q_2, q_3) of the quadratic function $L(a)$ of eqn (19) (Fig. 9). (d) Numerical values of the radius of curvature r_p of the proximal lens surface at the optical axis, (e-h) of the Gaussian constants ($g_{11}, g_{12}, g_{21}, g_{22}$), and (i) of the focal length L' measured from the proximal principal plane of the lens in the three stages of post-ecdysial development of Fig. 1 in *Phacops rana milleri*.

given lens thickness a the Huygensian profile varies from a conical, slightly incurved extreme form to a less curved and wavy extreme shape through a series of intermediate saucer-like profiles as L increases.

Comparing the shape of the proximal surface of the post-ecdysially developing lens of Fig. 1 with the family of curves of Fig. 7 we can establish that the theoretical conical, slightly incurved extreme forms, correspond to the shape of the proximal lens surface in stage (I) of post-ecdysial development [Fig. 1(a)], the other wavy extreme forms to stage (III) [Fig. 1(c)], and the theoretical saucer-like intermediate profiles to stage (II) [Fig. 1(b)].

6. Computational Reconstruction of a Probable Change of Form of the Developing Lens

Since the lens thickness a increased gradually during post-ecdysial development, a family of Huygensian profiles for a given value of a (Fig. 7) cannot, of course, represent the change of form of the developing lens. In order to reconstruct computationally a probable post-ecdysial development of the lens, we select those three theoretical Huygensian profiles from the family of curves of Fig. 7, which fit in best with the shape of the proximal lens surfaces of Fig. 1 as reconstructed by Miller & Clarkson (1980). This comparison is reliable, because the three different values of a in Fig. 7 are the same as those in Fig. 1 (see Table 1). The results of this selection are shown in Fig. 8; the fit is good. The three reconstructed values of L are given in Table 1.

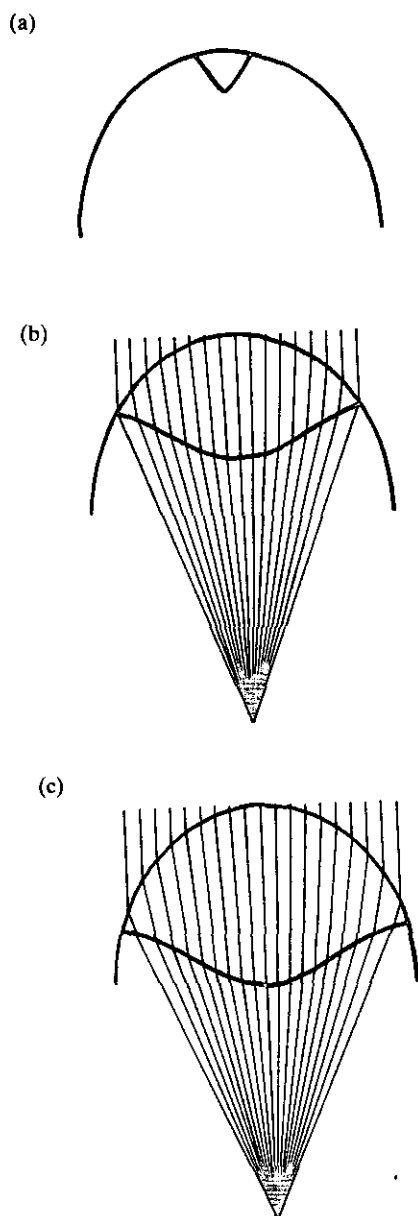


FIG. 8. Computationally reconstructed lenses in the post-ecdysially developing eye of *Phacops rana milleri* which fit best with the experimentally reconstructed real ones of Fig. 1. (a) $a_1 = 150 \mu\text{m}$, $L_1 = 50 \mu\text{m}$; (b) $a_2 = 450 \mu\text{m}$, $L_2 = 950 \mu\text{m}$; (c) $a_3 = 650 \mu\text{m}$, $L_3 = 850 \mu\text{m}$. Ray tracing through the lens is represented in cases (b) and (c).

Representing the related pairs $(L_i, a_i; i=1, 2, 3)$ of Table 1 in a system of coordinates, we obtain Fig. 9, on the basis of which function $L(a)$ can be approximated in the simplest continuous case by the quadratic expression

$$L(a) = q_1 + q_2 a + q_3 a^2 \quad (19)$$

with

$$\mathbf{q} = \mathbf{A}\mathbf{L}, \quad \mathbf{q} = (q_1, q_2, q_3), \quad \mathbf{L} = (L_1, L_2, L_3), \quad \mathbf{a} = (a_1, a_2, a_3),$$

$$\mathbf{A} = \frac{1}{J} \begin{pmatrix} a_2 a_3^2 - a_3 a_2^2 & a_3 a_1^2 - a_1 a_3^2 & a_1 a_2^2 - a_2 a_1^2 \\ a_2^2 - a_3^2 & a_3^2 - a_1^2 & a_1^2 - a_2^2 \\ a_3 - a_2 & a_1 - a_3 & a_2 - a_1 \end{pmatrix},$$

$$J = (a_2 - a_1)(a_3^2 - a_1^2) - (a_3 - a_1)(a_2^2 - a_1^2), \quad (20)$$

where the numerical value of components of vectors \mathbf{a} , \mathbf{L} and \mathbf{q} can be found in Table 1.

After the above empirical reconstruction of a possible relation between focal length and lens thickness during post-ecdysial development we reconstruct computationally a probable change of form of the developing lens. Using (19), (20) and data

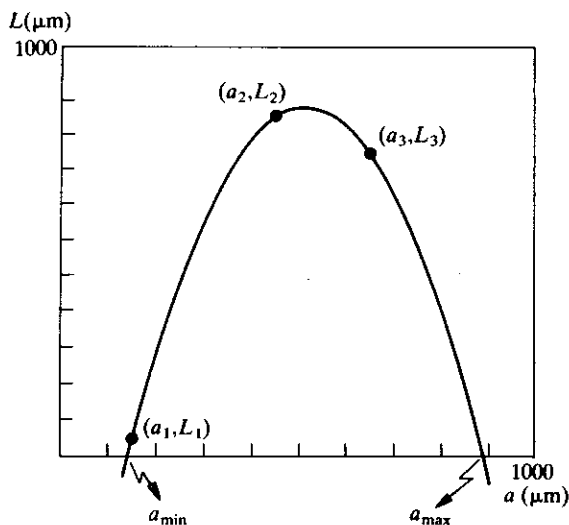


FIG. 9. Representation of the related pairs of the focal length L_i and the lens thickness a_i ($i=1, 2, 3$) of Table 1 (dots) and the graph of the quadratic function $L(a) = q_1 + q_2 a + q_3 a^2$ fitted to them. The numerical value of the parameters (q_1, q_2, q_3) can be found in Table 1. Interval $a_{\min} \leq a \leq a_{\max}$ is the domain of definition of our study.

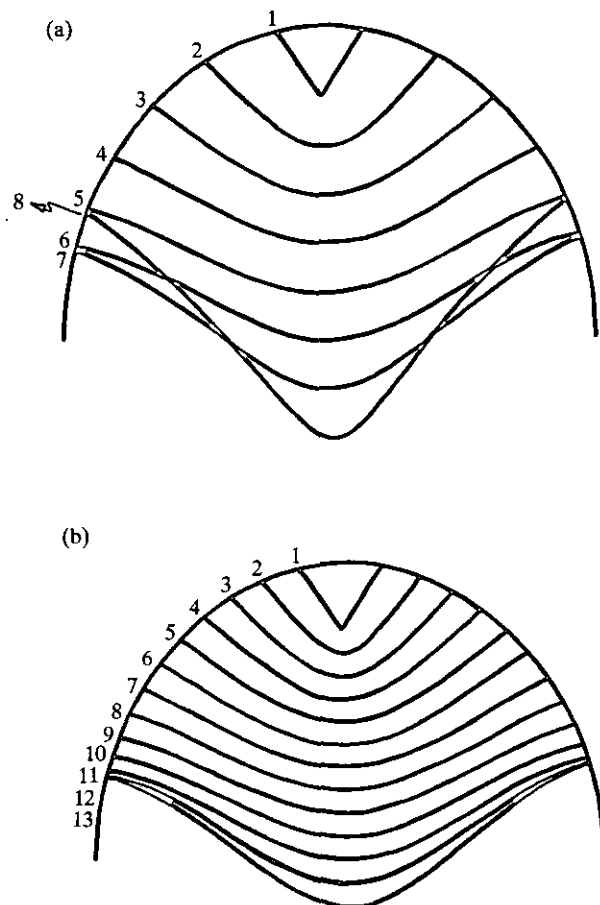


FIG. 10. Computational reconstruction of probable changes of form of the post-ecdysially developing lens in *Phacops rana milleri* as a function of the lens thickness a using function $L(a)$ described by (19) and represented in Fig. 9 with parameters (q_1, q_2, q_3) of Table 1. $a_i = a_0 + (i-1)\Delta a$, $i = 1, 2, \dots, N$; $a_0 = 142 \mu\text{m}$. (a) $\Delta a = 100 \mu\text{m}$, $N = 8$; (b) $\Delta a = 50 \mu\text{m}$, $N = 13$.

(q_1, q_2, q_3) of Table 1, we can determine how the proximal profile of the post-ecdysially developing singlet lens in *Phacops rana milleri* may have changed. The results are shown in Fig. 10.

7. Optical Features of Image Construction in the Post-ecdysially Developing Eye of *Phacops rana milleri*

7.1. DOMAIN OF SHARP VISION IN OBJECT SPACE

In order to characterize the probable optical features of image construction in the post-ecdysially developing eye of *Phacops rana milleri*, we investigate in this subsection object position and magnification of the developing singlet lens as a function

of the lens thickness and the position of the retina, supposing that the sharp image of an object falls on the retinal surface. The distance between the retina and the corneal surface is L_R , and the object is in front of the lens at a distance l_O^{sharp} from the distal lens surface. The post-ecdysially developing spherically corrected Huygenian singlet lens in *Phacops rana milleri* can be paraxially considered as a thick lens with spherical boundary surfaces of distal and proximal radius of curvature r_d and r_p , respectively. Therefore we can use in paraxial approximation the geometric optical formulae for spherical thick lenses. The Gaussian constants for the trilobite lens investigated are (Nussbaum & Phillips, 1976)

$$\mathbf{S} = \begin{pmatrix} g_{11} & -g_{12} \\ -g_{21} & g_{22} \end{pmatrix},$$

$$g_{11} = 1 - \rho_p \frac{a}{n_L},$$

$$g_{12} = \rho_d + \rho_p - \rho_d \rho_p \frac{a}{n_L},$$

$$g_{21} = -\frac{a}{n_L},$$

$$g_{22} = 1 - \rho_d \frac{a}{n_L}, \quad (21)$$

where \mathbf{S} is the system matrix of the lens, and ρ_d and ρ_p are the refracting power of the distal and proximal lens surface, respectively

$$\rho_d = \frac{n_L - n_w}{r_d}, \quad \rho_p = \frac{n_B - n_L}{r_p}, \quad r_d > 0, \quad r_p < 0. \quad (22)$$

The focal point F is at a distance

$$L = n_B \frac{g_{22}}{g_{12}} > 0 \quad (23)$$

from the proximal lens surface and at a distance

$$L' = \frac{n_B}{g_{12}} > 0 \quad (24)$$

from the proximal principal plane of the lens. The magnification M of the lens can be expressed as follows

$$M = g_{22} - g_{12} \frac{L_R - a}{n_B} = \frac{n_w}{n_w g_{11} + g_{12} l_O^{\text{sharp}}}, \quad (25)$$

from which the object position of sharp vision is

$$l_o^{\text{sharp}} = \frac{n_w}{g_{12}} \left[\frac{n_B}{n_B g_{22} - g_{12}(L_R - a)} - g_{11} \right] \leq 0. \quad (26)$$

From (21–23) one can obtain the expression of the radius of curvature of the proximal lens surface at the optical axis

$$r_p = \frac{L(n_B - n_L)[n_L r_d - a(n_L - n_w)]}{r_d n_L n_B - (n_B a + n_L L)(n_L - n_w)} < 0. \quad (27)$$

Using (18), one can determine the radius of curvature of the distal lens surface at the optical axis

$$r_d = \frac{[1 + f'(x=0)^2]^{3/2}}{|f''(x=0)|} = \frac{r^2}{d}. \quad (28)$$

We want to investigate l_o^{sharp} and M versus a and L_R , therefore we must first determine the domain of definition of a and L_R .

From the requirement $L(a) \geq 0$ an interval $a_{\min} \leq a \leq a_{\max}$ follows (see Fig. 9) as the domain of definition of the lens thickness, where

$$\begin{aligned} a_{\min} &= \frac{-q_2 + [q_2^2 - 4q_1 q_3]^{1/2}}{2q_3} = 140 \mu\text{m}, \\ a_{\max} &= \frac{-q_2 - [q_2^2 - 4q_1 q_3]^{1/2}}{2q_3} = 888 \mu\text{m}. \end{aligned} \quad (29)$$

However, we show later in the next section that our theoretical reconstruction may only be sound in the following smaller interval

$$a_{\min} = 140 \mu\text{m} \leq a \leq a_{\max} \approx 750 \mu\text{m}. \quad (30)$$

From the geometric requirements $l_o^{\text{sharp}} \leq 0$ and $L_R - a \geq L$ it follows that

$$L_R^{\min}(a) \equiv a + L(a) = q_1 + (1 + q_2)a + q_3 a^2 \leq L_R \leq L_R^{\max}(a),$$

where

$$L_R^{\max}(a) = a + n_B \frac{g_{11} g_{22} - 1}{g_{11} g_{12}} \equiv A \quad \text{if } A \geq 0,$$

and

$$L_R^{\max}(a) = +\infty \quad \text{if } A < 0. \quad (31)$$

For obvious anatomical reasons the retina, of course, could not be placed further from the corneal surface than an absolute maximum, the value of which can be estimated as

$$L_R \leq L_R^{\text{abs}} \approx 2000 \mu\text{m}. \quad (32)$$

On the basis of (30–32) the domain of definition in the plane (a, L_R) is represented in Fig. 11.

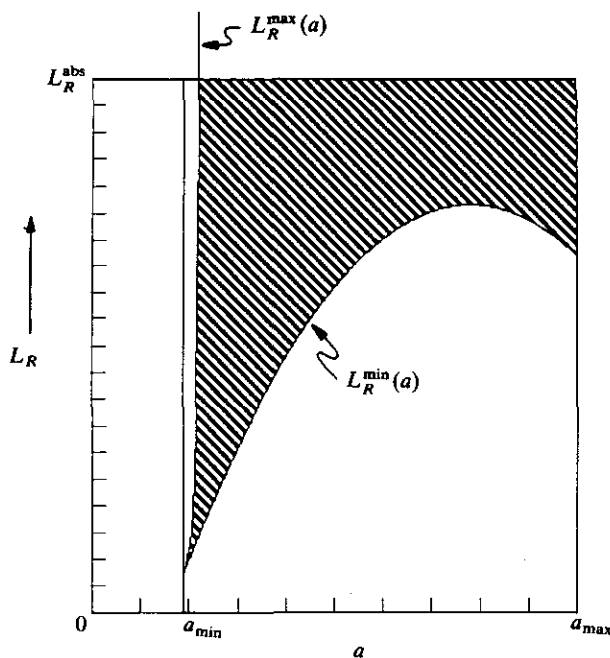


FIG. 11. Domain of definition (striped area) of our investigation in the plane of the lens thickness a and the distance of retina L_R from the corneal surface for calculation of object position l_O^{sharp} and magnification M of the post-ecdysially developing Huygenian singlet lens in the eye of *Phacops rana milleri*. Functions $L_R^{\text{min}}(a)$ and $L_R^{\text{max}}(a)$ are described by (31), $L_R^{\text{abs}} = 2000 \mu\text{m}$, $a_{\text{min}} = 140 \mu\text{m}$, $a_{\text{max}} = 750 \mu\text{m}$.

In Fig. 12(a) $\log(-l_O^{\text{sharp}})$ is shown as a function of a and L_R on the basis of (26). Figure 12(b) shows the contour-map of the three-dimensional surface of Fig. 12(a). One can see that approaching to the parabolic curve of $L_R^{\text{min}}(a)$, the object position $-l_O^{\text{sharp}}$ goes to infinity. In Fig. 13(a) the magnification M can be seen versus a and L_R on the basis of (25), and Fig. 13(b) shows the contour-map of this three-dimensional surface. The negative sign of magnification M means that the image is reversed. One can establish in Fig. 13 that the value of $|M|$ increases if L_R increases and/or a decreases.

7.2. ESTIMATION OF DEPTH OF FOCUS IN OBJECT SPACE

In this subsection we estimate the depth in object space over which the image was "in focus" in the post-ecdysially developing eye of *Phacops rana milleri*. We follow Land (1981) to derive an expression for depth of focus.

In the developing eye of *Phacops rana milleri* the distance l_O of an object from the corneal surface which is conjugate with an image at a distance l_I from the proximal lens surface is given by [see eqn (26)]

$$l_O = \frac{n_w}{g_{12}} \left[\frac{n_B}{n_B g_{22} - g_{12} l_I} - g_{11} \right] \leq 0. \quad (33)$$

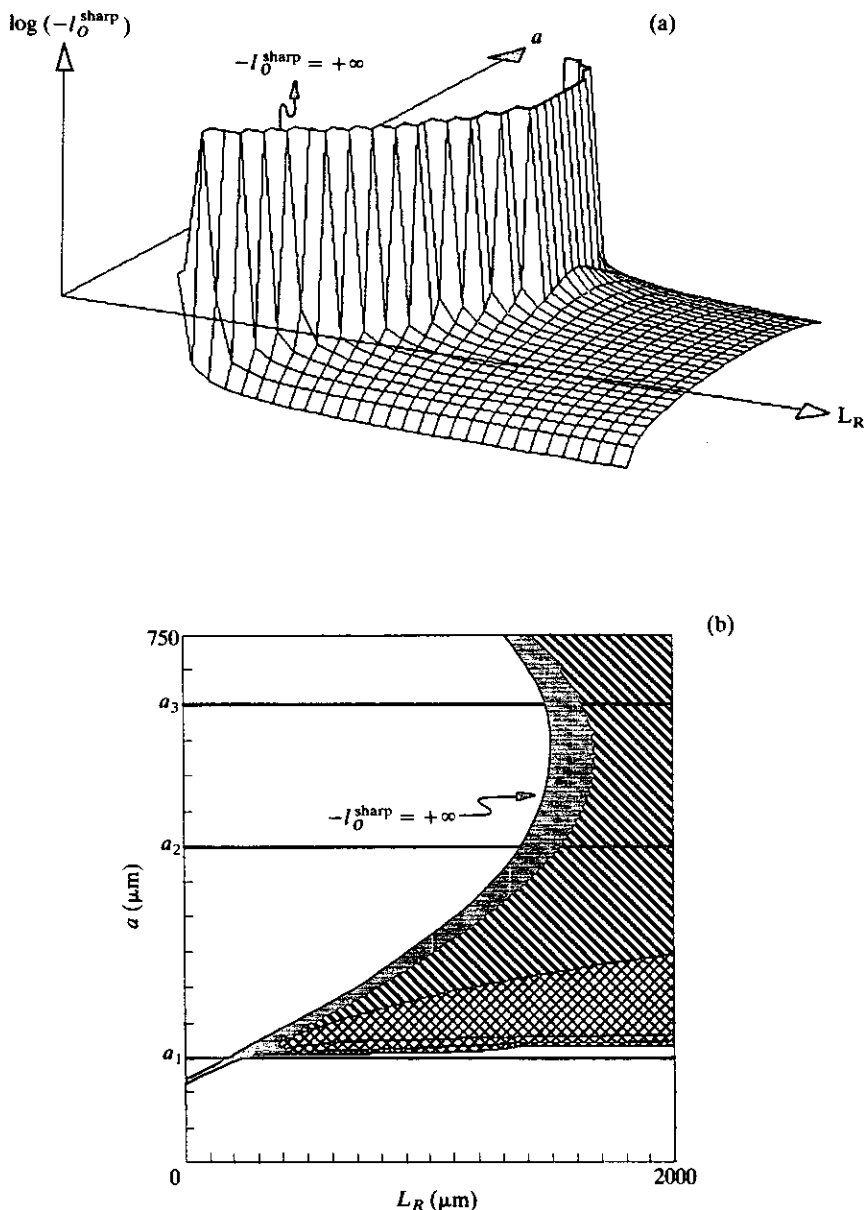


FIG. 12. (a) Three-dimensional representation of the logarithm of the object position $-l_o^{\text{sharp}}$ for sharp vision as a function of the lens thickness a and the distance L_R of retina from the corneal surface calculated for the post-ecdysially developing Huygensian singlet lens in the eye of *Phacops rana milleri*. The focal length L measured from the proximal lens surface varies versus a as the quadratic function $L(a)$ in Fig. 9 described by (19). If $L = L_R^{\text{min}}(a)$, then $\log(-l_o^{\text{sharp}}) = +\infty$. (b) Contour-map with contour-lines of different areas of the numerical value of object position $-l_o^{\text{sharp}}$ in the plane (L_R, a) for the domain of definition represented in Fig. 11. The left parabolic contour-line of the black-coloured area represents $-l_o^{\text{sharp}} = +\infty$. a_1 , a_2 and a_3 represent the lens thickness in the three stages of post-ecdysial development of Fig. 1. \square , $0 \leq -l_o^{\text{sharp}} \leq 1$ mm; \boxtimes , 1 mm $\leq -l_o^{\text{sharp}} \leq 1$ cm; \blacksquare , 1 cm $\leq -l_o^{\text{sharp}} \leq \infty$.

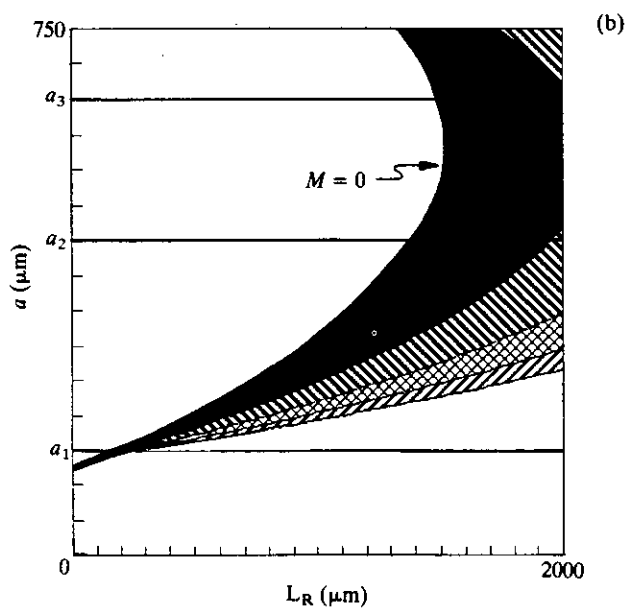
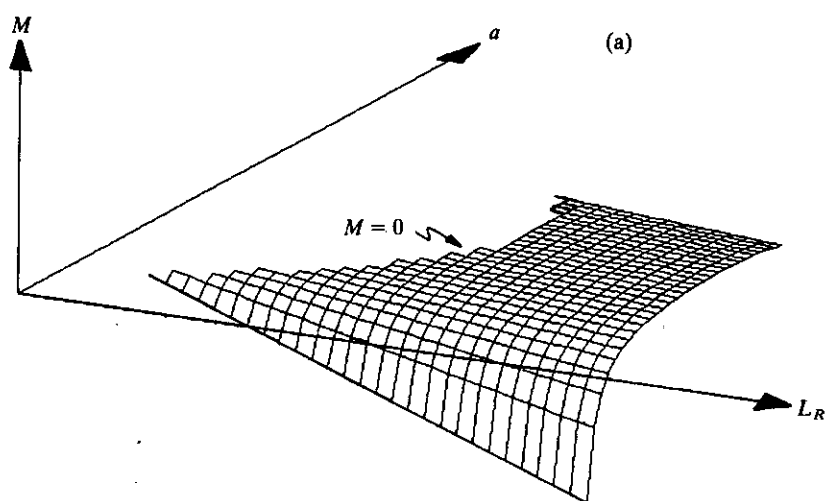


FIG. 13. As Fig. 12 for the magnification M . \square , $2 \leq -M$; diagonal lines , $1.5 \leq -M \leq 2$; cross-hatch , $1 \leq -M \leq 1.5$; horizontal lines , $0.5 \leq -M \leq 1$; \blacksquare , $0 \leq -M \leq 0.5$.

This expression can be used to find the depth in object space that produces a blur circle on the retina whose radius does not exceed a permitted amount (for example, the receptor separation). From Fig. 14, if an object at "far point" O_{far} forms an image at I_{far} and one at the "near point" O_{near} is imaged at I_{near} , the radius of the blur circle will be

$$r_{\text{blur}} = \sigma r_a \frac{L_R - a - l_I}{l_I + a - h},$$

$$h = d \left[1 - \sqrt{1 - \left(\frac{r_a}{r} \right)^2} \right] \quad (34)$$

when the object is either at the far point ($\sigma = +1$, $l_I = l_I^{\text{far}}$) or at the near point ($\sigma = -1$, $l_I = l_I^{\text{near}}$). Making r_{blur} equal to the receptor separation p in the retina, gives

$$l_I(a, L_R, \sigma, p) = \frac{\sigma r_a (L_R - a) - p[a - d + d\sqrt{1 - (r_a/r)^2}]}{p + \sigma r_a}. \quad (35)$$

Substituting for $l_I(a, L_R, \sigma, p)$ in (33) we obtain an expression for the object distance $l_O(a, L_R, \sigma, p)$. At the far, sharp and near point, respectively, the object distance is

$$l_O^{\text{far}} = l_O(a, L_R, \sigma = +1, p),$$

$$l_O^{\text{sharp}} = l_O(a, L_R, p = 0),$$

$$l_O^{\text{near}} = l_O(a, L_R, \sigma = -1, p). \quad (36)$$

The "exterior" and "interior" depth of focus is then defined as (see Fig. 14)

$$D_{\text{ex}} := l_O^{\text{sharp}} - l_O^{\text{far}} > 0 \quad \text{if } l_O^{\text{sharp}} \leq 0,$$

$$D_{\text{ex}} := -l_O^{\text{far}} > 0 \quad \text{if } l_O^{\text{sharp}} > 0 \text{ and } l_O^{\text{far}} \leq 0,$$

$$D_{\text{ex}} := 0 \quad \text{if } l_O^{\text{far}} > 0; \quad (37)$$

$$D_{\text{int}} := l_O^{\text{near}} - l_O^{\text{sharp}} > 0 \quad \text{if } l_O^{\text{near}} \leq 0,$$

$$D_{\text{int}} := -l_O^{\text{sharp}} > 0 \quad \text{if } l_O^{\text{near}} > 0 \text{ and } l_O^{\text{sharp}} \leq 0,$$

$$D_{\text{int}} := 0 \quad \text{if } l_O^{\text{sharp}} > 0. \quad (38)$$

Then the depth of focus can be defined as

$$D := D_{\text{ex}} + D_{\text{int}}. \quad (39)$$

The radius of aperture r_a can be determined during the calculation of the proximal Huygensian profile of the developing lens for a given lens thickness a .

Since the sublensar tissue has disappeared during fossilization and diagenesis, the value of receptor separation p can only be estimated. In its structure and optical optimization, the schizochroal dioptric apparatus recalls the ocellar eye of larvae of the sawfly *Perga* (Meyer-Rochow, 1974), therefore Campbell (1975) suggested that the sublensar tissue in schizochroal-eyed trilobites might also be similar to the ocellar

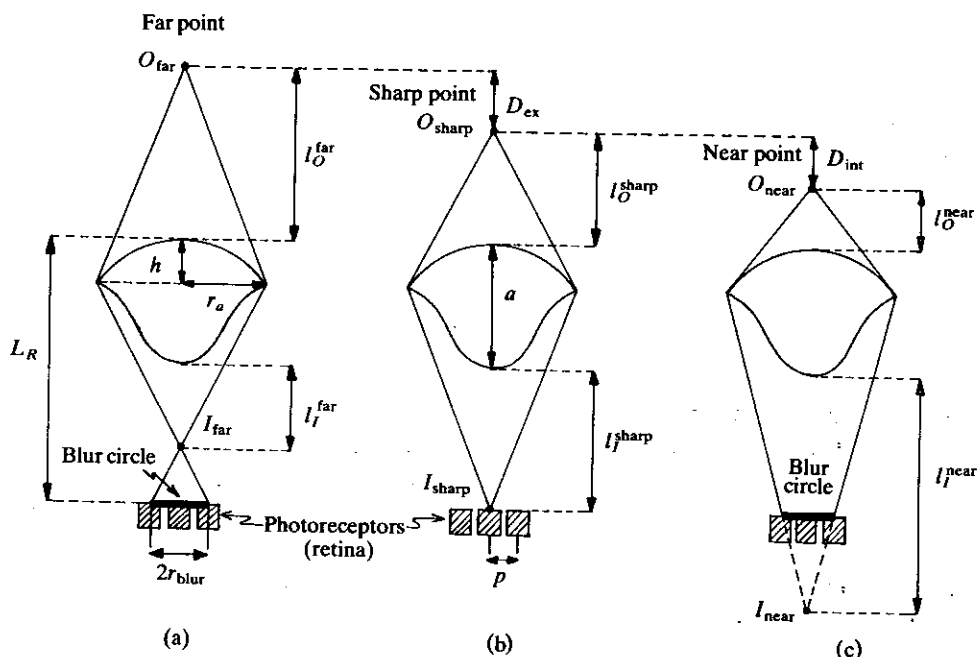


FIG. 14. Image construction in the post-ecdysially developing eye of *Phacops rana milleri* for calculation of depth of focus. Sharp vision (b) occurs when the image I_{sharp} of object point O_{sharp} falls on the retina. Then the radius of blur circle is zero ($r_{blur}=0$). If the image falls above (a) or below (c) the retina so that the radius of blur circle is smaller than the receptor separation p ($r_{blur} \leq p$), then objects between the "far point" O_{far} and the "near point" O_{near} can also sharply be seen by the retina. D_{ex} and D_{int} is the "exterior" and "interior" depth of focus in object space.

retina of sawfly larvae. Here, intertrabacular spacings are between 15 and 20 μm . Another candidate may be the pallial eye of scallop *Pecten* (Horváth & Varjú, 1993), in the distal retina of which the receptor separation is about 5 μm in the centre, and 10 μm towards the edges (Land, 1965, 1968). Therefore we calculate the exterior depth of focus for receptor separations 5, 10, 15 and 20 μm in the developing eye of *Phacops rana milleri*. In Fig. 15 the contour-map of the three-dimensional surface of $\log(D_{ex})$ is shown versus a and L_R for $p=5, 10, 15$ and 20 μm on the basis of (33) and (35–37).

We have supposed during the above derivation that the retina of *Phacops rana milleri* was a single plane of negligible depth. This was true if the receptors were short or if they were long but were optically isolated from each other (Land, 1981).

8. Discussion

In terms of the above analysis we may conclude the following.

(i) Some theoretically calculated Huygensian profiles (Fig. 8) fit in well with the shape of the proximal surface of the post-ecdysially developing singlet lens in the schizochroal compound eye of the trilobite *Phacops rana milleri* as reconstructed

earlier by Miller & Clarkson (1980) (Fig. 1). It thus seems pertinent to suppose that the conical, slightly incurved form of the proximal surface of the lens in the very early post-ecdysial stage (I) [Figs 1(a) and 8(a)] and the saucer-like, less curved shape of the proximal lens surface in the later stage (II) of development [Figs 1(b) and 8(b)] in the eye of *Phacops rana milleri* were likewise optimized for correction of spherical aberration of the lens, as was the wavy proximal Huygensian profile at the later stage (III) [Figs 1(c) and 8(c)].

From this it is clear that question (a) in the Introduction is answered positively: the post-ecdysial lenses were optically optimized in all stages of development.

(ii) On the basis of the three data pairs (L_i, a_i ; $i = 1, 2, 3$) of Table 1 (Fig. 9) the quadratic expression (19) can be derived as the simplest continuous form of variation of focal length L versus lens thickness a , which makes it possible to reconstruct computationally a probable series of shapes of the post-ecdysially developing lens in the eye of *Phacops rana milleri* [Fig. 10(b)].

This answers question (c) as propounded in the Introduction.

In stage (IV) of the post-ecdysial development of the lens a transition took place from the homogeneous singlet lens with its wavy Huygensian proximal profile to the more complex, heterogeneous mature doublet form of stage (V) with its core and intralensar bowl. In order that the bowl-shaped proximal surface can develop after stage (IV), thickening of the lens must stop at the periphery whilst continuing centrally, until its thickness reached that of the upper unit of the mature lens.

In Fig. 10(a) we can see that our computational reconstruction based on (19) (Fig. 9) results also in conical proximal Huygensian lens profiles for larger values of lens thickness a because of the decreasing part of the quadratic function $L(a)$. Of course, the proximal growth of the lens, that is, accretion of new material on the proximal lens surface must have been irreversible, therefore profile 8 of Fig. 10(a) must be rejected, because this requires reversal of growth peripherally. From this we deduce that the quadratic function (19) becomes valid for $a > a_4 \approx 750 \mu\text{m}$. The development of the lens shape is shown in Fig. 10(b), on the basis of which we propose a possible means whereby the lens passed through the transitional stage (IV) as follows.

(iii) After the wavy Huygensian profile of stage (III) took shape, proximal accretion of new material ceased at the periphery of the lens but continued at the same rate centrally until the thickness reached the value $a_4 \approx 750 \mu\text{m}$ [see Fig. 10(b)]. Thus far the lens has been corrected for spherical aberration. With further development it generally changed to become bowl-shaped, and of very different form to the ideal Huygensian profile. At this point there is a dramatic, though temporary, loss of optical quality. Until the core has differentiated and the intralensar bowl has been added to the upper lens unit, that is, until the fully mature form has taken shape, the optimized function of the lens must have been reduced, and its image formation must correspondingly have been poor.

This conclusion answers question (d) of the Introduction.

Disregarding the central core, the structure of the doublet mature lens in *Phacops rana milleri* is similar to that of other phacopid trilobites as *Crozonaspis struvei* or *Dalmanitina socialis*, for example, which had highly optimized schizochroal lenses corrected for spherical aberration (Clarkson & Levi-Setti, 1975; Horváth, 1989a). This

similarity supports the view that the mature eye of *Phacops rana milleri* was optimized, too, but the optical function of the core in the upper lens unit remains unknown, and further studies are required to elucidate it.

From (29) it follows that there must have been a minimal lens thickness a_{\min} , below which the developing visual system of *Phacops rana milleri* could not have been optimized. Similarly there is a maximal lens thickness a_{\max} above which the developing eye could not have been aplanatic. In all likelihood, however, the quadratic form (19) of function $L(a)$ becomes valid, that is, our computational reconstruction and the optimized optical function of the proximal Huygensian lens profile would have been sound in the range of $140 \mu\text{m} \leq a \leq 750 \mu\text{m}$ until the transitional stage (IV) has been reached as we assumed in conclusion (iii).

The original sublensar structures have disappeared during fossilization and diagenesis, therefore nothing certain can be established above the distance L_R of the retina (if any) from the corneal surface in trilobite eyes. Clarkson & Levi-Setti (1975) estimated that in a simple model of *Crozonaspis struvei* the focal length of the lens was about equal to its thickness, measured from the proximal surface of the lens. Campbell (1975) suggested a focal length near 1.6 times the thickness of the lens. Stockton & Cowen (1976) calculated that in a typical member of the Phacopina the retina would have lain perhaps 1 mm behind the lens, and with its supporting sclera would have occupied most of the diameter of the lens barrel.

Campbell (1975), on the basis of analogies with living arthropods possessing ocellar eyes, reached the same conclusion. Further support for this argument comes from Clarkson's (1967, 1969) observation of sublensar cones or cylinders in *Phacops secundus* and *Reedops cephalotes*. These would have contained tissues or fluids and may have been floored by a retina. Integrative neural tissue would have lain behind the sublensar cylinder. Horváth (1989a) calculated that the focal point must have been at a distance of about 170 μm , 210 μm and 230 μm from the proximal lens surface in the schizochroal eye of *C. struvei*, *D. socialis* and a Silurian *Dalmanites*, respectively, in order to take advantage of their optimized doublet lenses. These arguments suggest that cylindrical structures of significant length probably lay behind each lens of the schizochroal trilobite eye.

There is no conclusive evidence as to the precise location of the retina behind the lens, and unless such is yielded by further studies of fossil material there must always remain some doubt. It is, however, possible to calculate the positions of the retina where schizochroal-eyed trilobites could take advantage of their spherically corrected lenses. In order to determine these retinal positions in the post-ecdysially developing eye of *Phacops rana milleri*, we studied the object position l_o^{sharp} and the magnification M of its developing Huygensian singlet lenses as a function of the lens thickness a and the distance of the retina L_R from the corneal surface. The results are shown in Figs 12 and 13, and in Table 2.

It is evident, for example [Fig. 12(b) and Table 2], that at stage II [Fig. 1(b)] of post-ecdysial development *Phacops rana milleri* could see sharply an object in front of its eye at a distance of $3 \text{ mm} \leq -l_o^{\text{sharp}} \leq 1 \text{ cm}$ with magnification $0.12 \leq -M \leq 0.54$, if its retina was placed at a distance $1534 \mu\text{m} \leq L_R \leq 2000 \mu\text{m}$ from the corneal surface. In order to see sharply an object at a distance $1 \text{ cm} < -l_o^{\text{sharp}} \leq \infty$ the position of the

TABLE 2

*Intervals of the distance L_R of retina from the corneal surface and the corresponding intervals of the calculated object position l_O^{sharp} and magnification M of the Huygensian singlet lens of *Phacops rana milleri* in the three stages of development of Fig. 1 (see Figs 12 and 13)*

Lens 1 Stage (I) of Fig. 1(a)	Lens 2 Stage (II) of Fig. 1(b)	Lens 3 Stage (III) of Fig. 1(c)
$200.3 \mu\text{m} \leq L_R \leq 238.3 \mu\text{m}$	$1534 \mu\text{m} \leq L_R \leq 2000 \mu\text{m}$	$1623 \mu\text{m} \leq L_R \leq 2000 \mu\text{m}$
$0 \leq -l_O^{\text{sharp}} \leq 1 \text{ cm}$	$3 \text{ mm} \leq -l_O^{\text{sharp}} \leq 1 \text{ cm}$	$3 \text{ mm} \leq -l_O^{\text{sharp}} \leq 1 \text{ cm}$
$0.00571 \leq -M \leq 0.7292$	$0.1207 \leq -M \leq 0.5405$	$0.1146 \leq -M \leq 0.4657$
	$1412 \mu\text{m} < L_R < 1534 \mu\text{m}$	$1511 \mu\text{m} < L_R < 1623 \mu\text{m}$
	$1 \text{ cm} < -l_O^{\text{sharp}} < 10 \text{ cm}$	$1 \text{ cm} < -l_O^{\text{sharp}} < 10 \text{ cm}$
	$0.01081 < -M < 0.1207$	$0.01025 < -M < 0.1146$
$200 \mu\text{m} \leq L_R < 200.3 \mu\text{m}$	$1400 \mu\text{m} \leq L_R \leq 1412 \mu\text{m}$	$1500 \mu\text{m} \leq L_R \leq 1511 \mu\text{m}$
$1 \text{ cm} < -l_O^{\text{sharp}} \leq \infty$	$10 \text{ cm} \leq -l_O^{\text{sharp}} \leq \infty$	$10 \text{ cm} \leq -l_O^{\text{sharp}} \leq \infty$
$0 \leq -M < 0.00571$	$0 \leq -M \leq 0.1081$	$0 \leq -M \leq 0.01025$

retina must have remained within the black-coloured area of Fig. 12(b) during post-ecdysial development, that is, the retina must have been placed from the corneal surface at a distance (see Table 2) $200 \mu\text{m} \leq L_R \leq 200.3 \mu\text{m}$, $1400 \mu\text{m} \leq L_R \leq 1534 \mu\text{m}$ and $1500 \mu\text{m} \leq L_R \leq 1623 \mu\text{m}$, respectively, in stages (I), (II) and (III) of development (Fig. 1).

This means that to make use of the Huygensian singlet lenses in this interval of object position, the retina would have to abandon its location and move backward by about $1200 \mu\text{m}$ between stages (I) and (II), and by about $100 \mu\text{m}$ between stages (II) and (III). During this time the magnification would have remained between $0 \leq -M \leq 0.5$. We do not know of any equivalent change of retinal position as great as $1200 \mu\text{m}$ in any modern arthropod, and we do not think it happened in trilobites either. It is difficult to envisage how the retina could be shifted relative to the lens, unless there were some muscular mechanism at the back but, as we have shown, this does not matter much for objects relatively close to the eye. It is, however, biologically imaginable that the position of the retina relative to the lens could have altered by $100 \mu\text{m}$ between stages (II) and (III).

Similar moveable retina can be found in the anterior median eyes of spiders, for example, whose eyes are capable of detailed image formation, have small visual fields, function at moderate distances, and are used for object fixation (Waterman, 1981). Another possibility for accommodation is to have a multiple retinal layer. Four reticular cell types with different spectral sensitivities were found in the salticid jumping spider *Menemerus* (Yamashita & Tateda, 1976), for example, where some support was inferred for the segregation of different types in four retinal layers as earlier proposed on optical grounds (Land, 1969).

These considerations, however, pertain to *Phacops rana milleri* focusing sharply on distance in the range of object position $1 \text{ cm} < -l_o^{\text{sharp}} \leq \infty$. However, it is more likely that during the post-ecdysial period, when *Phacops rana milleri* needed to keep out of sight, possibly by partial burial or by hiding, it might be sufficient to see sharply objects within the range of *a few millimetres* $\leq -l_o^{\text{sharp}} \leq \text{a few centimetres}$. In this case the retina must have been lain within the striped area or near the right border of the black-coloured area in Fig. 12(b) and, except for very small values of the lens thickness a , it need not move either backward nor forward and need not have multiple layers.

If the retinal distance did not change, sharp vision of *Phacops rana milleri* must have been myopic in the very early stages of post-ecdysial development [in stage (I), for example], later becoming gradually emmetropic [in stages (II) and (III), for example]. For larger values of a than $a_3 = 650 \mu\text{m}$ the sharp vision of *Phacops rana milleri* would have become again a little myopic but remaining in the range of *a few millimetres* $\leq -l_o^{\text{sharp}} \leq \text{a few centimetres}$; furthermore, as we mentioned above in conclusion (iii), the optimized function of the lens must have been reduced for lenses thicker than about $750 \mu\text{m}$. It is now possible to reach the following conclusions.

(iv) In order to take advantage of the spherically corrected Huygensian singlet lenses during post-ecdysial development, the position of the retina in the eye of *Phacops rana milleri* must have fallen within the biologically reliable striped area or near the right border of the black-coloured area of Fig. 12(b), supposing that the emmetropic sharp vision in the post-ecdysial period can be characterized by *a few millimetres* $\leq -l_o^{\text{sharp}} \leq \text{a few centimetres}$. Furthermore, supposing that the position of the single-layered retina did not change, the vision of *Phacops rana milleri* was myopic in the very early stages of development. In point of fact the possession of a small, conical Huygensian lens in stage (I) might not have conferred a very great optical advantage. Later, as the lens thickened the vision became progressively emmetropic and *Phacops rana milleri* could make use of its spherically corrected Huygensian singlets. Prior to developmental stage (IV) as described in conclusion (iii), the vision became again a little myopic, but *Phacops rana milleri* could still see sharply within the region of *a few millimetres* $\leq -l_o^{\text{sharp}} \leq \text{a few centimetres}$. During post-ecdysial development the magnification $-M$ of the reversed retinal image decreased gradually from two to near zero, as can be read in Fig. 13(b).

(v) It is possible that the initial conical shape of the small developing calcite lens of stage (I) may have little to do with optics, and the fact that its shape is consistent with a Huygensian correction for spherical aberration is only an accidental coincidence. In the later developmental stages, however, this is certainly not true, and *Phacops rana milleri* could make use of its Huygensian singlet lenses in the range of object position from a few millimetres to a few centimetres. The correction for spherical aberration, therefore, would give the eye relatively sharp and bright vision throughout the whole post-ecdysial period, except perhaps for the very early developmental stage.

These latter two conclusions answer question (b) of the Introduction.

In order to estimate the depth in object space over which the image was in focus in the developing eye of *Phacops rana milleri*, we investigated the exterior depth of

focus D_{ex} as a function of receptor separation p in the retina. From Fig. 15 one can read that if the receptor separation in the eye of *Phacops rana milleri* was similar to that of scallop *Pecten* ($5 \mu\text{m} \leq p \leq 10 \mu\text{m}$) or sawfly larva *Perga* ($15 \mu\text{m} \leq p \leq 20 \mu\text{m}$) and the position of *Phacops*' retina has fallen near the right border of the black-coloured area of Fig. 12(b), then the exterior depth of focus of the developing eye was $1 \text{ mm} \leq D_{ex} \leq 1 \text{ cm}$ (see Fig. 15 for $p = 5$ and $10 \mu\text{m}$) or $1 \text{ mm} \leq D_{post} \leq 1 \text{ dm}$ (see Fig. 15 for $p = 15$ and $20 \mu\text{m}$), respectively.

From (34) it is clear that decreasing the radius of aperture r_a of the lens, also decreases the radius of blur circle that is, the depth of focus increases. It is well known how depth of focus can dramatically improve when a small lens aperture is used in photographic equipment—a very useful principle when photographing highly convex objects, for example. If there were an annular pigment sleeve below the lens

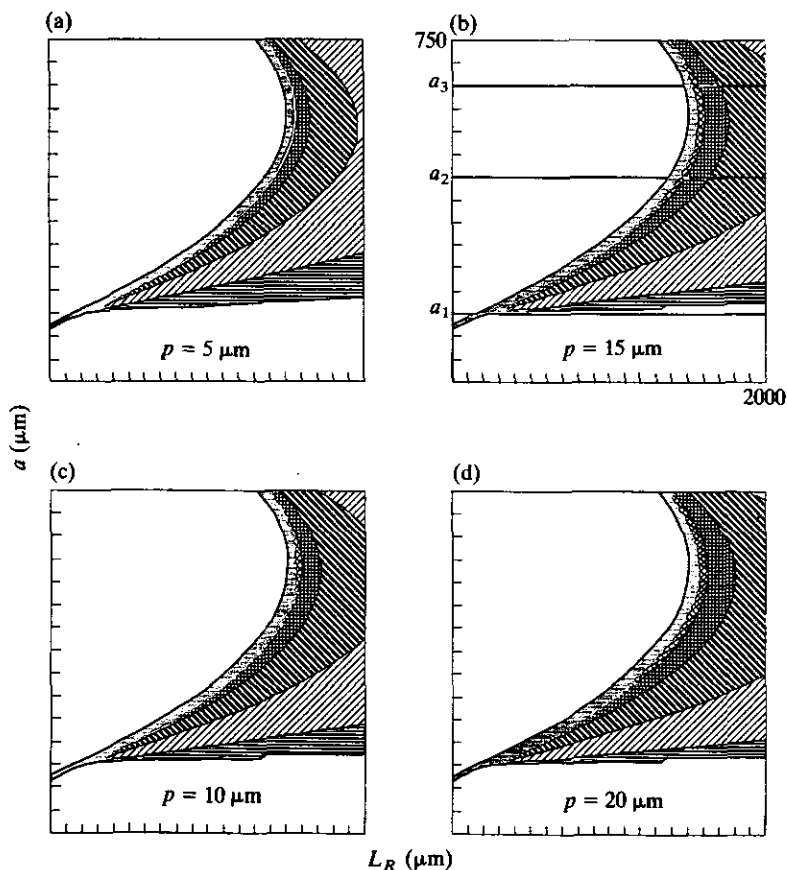


FIG. 15. As Fig. 12(b) for the exterior depth of focus D_{ex} (see Fig. 14) for receptor separations $p = 5, 10, 15$ and $20 \mu\text{m}$. \square , $1 \mu\text{m} \leq D_{ex} \leq 10 \mu\text{m}$; \square , $10 \mu\text{m} \leq D_{ex} \leq 100 \mu\text{m}$; \square , $100 \mu\text{m} \leq D_{ex} \leq 1 \text{ mm}$; \square , $1 \text{ mm} \leq D_{ex} \leq 1 \text{ cm}$; \blacksquare , $1 \text{ cm} \leq D_{ex} \leq 10 \text{ cm}$; \blacksquare , $10 \text{ cm} \leq D_{ex} \leq \infty$.

of *Phacops rana milleri* (analogous to the diaphragm of a camera lens) this would help in improving depth of field in the developing eye.

Such a diaphragm would be broadly analogous to the opaque ring of pigment present in dark-adapted superposition eyes. In the light-adapted superposition eye (for example, Debasieux, 1944), a cylinder of pigment surrounds each ommatidium below the level of the lens, thus screening it from its neighbours. When the eye is adapted to dark conditions the pigment withdraws proximally and distally, thereby allowing the light to reach many photoreceptors rather than just one. There is thus a pigment ring below each lens, when the eye is dark adapted, and whereas its primary function is not that of a diaphragm, it could be pre-adapted for such use. But the early conical lens of *Phacops rana milleri* is of such a different shape to standard lenses, and so small in any case, that we do not know whether such a principle would apply.

Towe (1973) has tested the optics of mature corneal lenses of the holochroal-eyed trilobite *Isotelus gigas* and the schizochroal-eyed trilobite *Phacops rana*. His microscopical experimentation revealed that all objects appeared to remain in focus for the human eye from a distance of just a few millimetres up to infinity with no change in the position of the microscope objective required. From this Towe (1973) concluded that the biconvex lenses of trilobites were able to form inverted, sharp images over a wide depth of field.

From this we conclude the following:

(vi) Supposing that the receptor separation in the retina of *Phacops rana milleri* was 5–10 μm or 15–20 μm and the position of retina has fallen near the right border of the black-coloured area of Fig. 12(b), the exterior depth of focus of the post-ecdysially developing eye was about 1 cm or 1 dm, respectively. The depth of field, of course, increases the range of sharp vision (a few millimetres—a few centimetres) as determined above theoretically. Therefore it is pertinent to suppose that *Phacops rana milleri* might see objects sharply over several centimetres, perhaps about 1 dm, with its post-ecdysially developing eyes.

Miller & Clarkson (1980) earlier supposed that the optical function of the lens optimized gradually as the lens developed and as the components within it differentiated. In their opinion the eye must have reached maximum efficiency only when the cuticle had achieved its full thickness. The time scale of this process is not known, but the thickness of the cuticle is such that it must have been some time, perhaps even several days after ecdysis, before visual acuity could be returned to an optimal level. This seems to have been, at least to some extent, a limitation on trilobite organization to add to those occasioned by ecdysis itself. The conical shape of the early lenses apparently was retained only during the period while the cuticle was flexible, so that the trilobite would not have been capable of much movement. In this state the animal probably had to hide, as do many newly ecdysed arthropods.

Miller & Clarkson (1980) thought that although there is not an exact equivalence, these conical lenses resemble the parabolic exocoines of *Limulus* described by Levi-Setti *et al.* (1975) as ideal light concentrators. They believed that for a recently moulted trilobite, which needed to keep out of sight (possibly either by partial burial

or by timing ecdysis at night-time), there would be a great value in having eyes highly sensitive to light for detection of potential enemies. The conical lenses could therefore have been optimized, at this early and most critical stage, for the best possible vision given their incomplete formation. In their opinion the early lens shapes were certainly not ideal, neither in terms of their construction nor of economy of material, and in the later stages of development change in optical function is reflected in the change of the lens shape.

However, our present analysis of the optics of the developing eye of *Phacops rana milleri* in this work puts the matter in a new light. As we have shown above, except for the small conical lens of stage (I), the optical function of the lens of *Phacops rana milleri* would have been already optimized at the early stages of development, and would have reached the maximum efficiency possible by using Huygensian proximal lens surface for correction of spherical aberration, so increasing its light-collecting efficiency and transfer of contrast.

Levi-Setti *et al.* (1975) suggested that focusing might occur by reflection from the walls of the crystalline cones. They pointed out that the shape of the cones resembled that of an ideal collector, a reflecting device originally designed for the collection of faint radiation. Land (1979, 1980), however, showed that focusing occurs in the cones of *Limulus* not by reflection—as Levi-Setti *et al.* (1975) supposed—but by inhomogeneous refraction. The refractive index gradient in the *Limulus* cornea, measured by interference microscopy, is precisely that required for lens-cylinder optics (Land, 1979).

The method of light-collection in the very early conical lenses of stage (I) in *Phacops rana milleri* differs from that of the crystalline cone of *Limulus*. *Phacops* achieved an increase of light-collecting efficiency in the focal plane exclusively by refraction on the distal corneal and the proximal Huygensian boundary surfaces of its lens, but *Limulus* by inhomogeneous refraction through the whole dioptric apparatus (Land, 1979, 1980). However, as we showed above, *Phacops rana milleri* could not optically make full use of this small conical calcite lens, because of its very small focal length.

Though the shape of the proximal surface of the lens changed in the later stages of development, this may not reflect the change in optical function (that is, increasing the light-collecting efficiency by Huygensian proximal lens surfaces) but rather the change of lens thickness and its focal length in accordance with the fine tuning between them supposed, and described by (19).

The compound eyes of trilobites are of particular interest because the trilobite eye is the most ancient visual system so far known. Earlier, Miller & Clarkson (1980) sought to explore the developmental process of post-ecdysial maturation in the schizochroal compound eye of *Phacops rana milleri*. The present study makes it possible that this maturation took place through more developmental stages characterized by a relatively high degree of optical optimization.

The optical maturation of *Phacops rana milleri* differs from that found in the dioptric apparatus in some modern compound eyes. One can refer, for example, to a recent study on the maturation of optics and resolution of the superposition eyes in the nocturnal adult dung beetle *Onitis aygulus* (Warrant *et al.*, 1990).

In the case of this beetle the image quality is poor immediately following ecdysis. As the eye matures, the lenses become more powerful, so that the position of best focus is shifted distally and the distribution of rays becomes spatially sharper. By the end of the first week after ecdysis, the lenses have matured sufficiently to shift the position of best focus to be coincident with the retinal surface. After this time, further maturation of the lenses is restricted to fine tuning of the refractive index gradients.

The slow maturation of optics and resolution in the dung beetle *O. aygulus* (Warrant *et al.*, 1990) is different from the maturation of optics through relatively highly optimized post-ecdysial stages presented in Miller & Clarkson (1980) and in this work for the trilobite *Phacops rana milleri*, and probably the reason for this difference can be attributed to the different post-ecdysial life styles of the two animals.

Thanks are due to an anonymous referee, who brought our attention to the problem of object position and depth of focus depending on the distance of retina from the corneal surface in an earlier version of the manuscript. Financial support came for G.H. from the *Bayerisches Staatsministerium für Unterricht, Kultus, Wissenschaft und Kunst* (Munich). Some results of this work originated during the scholarship received by G.H. in the Institute for Zoology, Department of Professor D. Burkhardt, University of Regensburg.

REFERENCES

- CAMPBELL, K. S. W. (1975). The functional anatomy of trilobites: musculature and eyes. *J. Proc. R. Soc. N.S.W.* **108**, 168–188.
- CLARKSON, E. N. K. (1966a). Schizochroal eyes and vision of some Silurian acastid trilobites. *Palaeontology* **9**, 1–29.
- CLARKSON, E. N. K. (1966b). Schizochroal eyes and vision of some phacopid trilobites. *Palaeontology* **9**, 464–487.
- CLARKSON, E. N. K. (1967). Fine structure of the eye in two species of *Phacops* (Trilobita). *Palaeontology* **10**, 603–616.
- CLARKSON, E. N. K. (1968). Structure of the eye of *Crozonaspis struvei* (Trilobita, Dalmanitidae, Zeliszkeellinae). *Senckenberg. lëth.* **49**, 383–391.
- CLARKSON, E. N. K. (1969). On the schizochroal eyes of three species of *Reedops* (Trilobita, Phacopidae) from the Lower Devonian of Bohemia. *Trans. R. Soc. Edin.* **68**, 183–205.
- CLARKSON, E. N. K. (1971). On the early schizochroal eyes of *Ormathops* (Trilobita, Zeliszkeellinae). *Mem. Bur. Rech. géol. minières (Fr.)* **73**, 51–63.
- CLARKSON, E. N. K. (1973). Morphology and evolution of the eye in Upper Cambrian *Olenidae* (Trilobita). *Palaeontology* **16**, 735–763.
- CLARKSON, E. N. K. (1975). The evolution of the eye in trilobites. *Fossils Strata* **4**, 7–31.
- CLARKSON, E. N. K. (1979). The visual system of trilobites. *Palaeontology* **22**, 1–22.
- CLARKSON, E. N. K. & LEVI-SETTI, R. (1975). Trilobite eyes and the optics of DesCartes and Huygens. *Nature, Lond.* **254**, 663–667.
- DEBASIEUX, P. (1944). Les yeux des crustacés: structure, développement, réactions à l'éclairement. *La Cellule* **50**, 5–122.
- DES CARTES, R. (1637). *Oeuvres de DeCartes. La Géométrie*, Livre 2. pp. 134. Leyden: J. Maire.
- ELDRIDGE, N. (1972). Systematics and evolution of *Phacops rana* (Green, 1832) and *Phacops iowensis* (Delo, 1935) (Trilobita) from the Middle Devonian of North America. *Bull. Am. Mus. Nat. Hist.* **147**, 45–113.
- FEIST, R. & CLARKSON, E. N. K. (1989). Environmentally controlled phyletic evolution, blindness and extinction in Late Devonian tropidocoryphine trilobites. *Lethaia* **22**, 359–373.
- FORDYCE, D. & CRONIN, T. W. (1989). Comparison of fossilized schizochroal compound eyes of phacopid trilobites with eyes of modern marine crustaceans and other arthropods. *J. Crust. Biol.* **9**, 554–569.

- HORVÁTH, G. (1989a). Geometric optics of trilobite eyes: theoretical study of the shape of aspherical interface in the cornea of schizochroal eyes of phacopid trilobites. *Math. Biosci.* **96**, 79–94.
- HORVÁTH, G. (1989b). Geometric optical optimization of the corneal lens of *Notonecta glauca*. *J. theor. Biol.* **139**, 389–404.
- HORVÁTH, G. & GREGUSS, P. (1989a). Geometrical optics of the corneal lens of backswimmer, *Notonecta glauca*. *Appl. Optics* **28**, 1974–1976.
- HORVÁTH, G. & GREGUSS, P. (1989b). Biooptical study of the corneal lens of the water bug *Notonecta glauca*. *Int. Agrophys.* **5**, 231–246.
- HORVÁTH, G. & VARJÚ, D. (1993). Theoretical study of the optimal shape of the front profile of the lens in the eye of the scallop, *Pecten*. *Bull. math. Biol.*, **55**, 155–174.
- HUYGENS, C. (1690). *Traité de la Lumière*. Leyden: Pierre van der Aa.
- LAND, M. F. (1965). Image formation by a concave reflector in the eye of the scallop, *Pecten maximus*. *J. Physiol.* **179**, 138–153.
- LAND, M. F. (1968). Functional aspects of the optical and retinal organization of the mollusc eye. *Symp. Zool. Soc. Lond.* **23**, 75–96.
- LAND, M. F. (1969). Structure of the retinæ of the principal eyes of jumping spiders (Salticidae: Dendryphantinae) in relation to visual optics. *J. exp. Biol.* **51**, 443–470.
- LAND, M. F. (1979). The optical mechanism of the eye of *Limulus*. *Nature, Lond.* **280**, 396–397.
- LAND, M. F. (1980). Compound eyes: old and new optical mechanisms. *Nature, Lond.* **287**, 681–686.
- LAND, M. F. (1981). Optics and vision in invertebrates. In: *Comparative Physiology and Evolution in Invertebrates. B: Invertebrate Visual Centers and Behavior I. Handbook of Sensory Physiology VII/6B*. (Autrum, H., ed.) pp. 471–592. Berlin: Springer Verlag.
- LEVI-SETTI, R., PARK, D. A. & WINSTON, R. (1975). The corneal cones of *Limulus* as optimised light concentrators. *Nature, Lond.* **253**, 115–116.
- MEYER-ROCHOW, V. B. (1974). Structure and function of the larval eye of the sawfly, *Perga*. *J. Insect Physiol.* **20**, 1565–1591.
- MILLER, J. & CLARKSON, E. N. K. (1980). The post-ecdysial development of the cuticle and the eye of the Devonian trilobite *Phacops rana milleri* Stewart 1927. *Proc. R. Soc. Lond. B* **288**, 461–480.
- NUSSBAUM, A. & PHILLIPS, R. A. (1976). *Contemporary Optics for Scientists and Engineers*. pp. 511. Englewood Cliffs, NJ: Prentice-Hall.
- SCHWIND, R. (1980). Geometrical optics of the *Notonecta* eye: adaptations to optical environment and way of life. *J. Comp. Physiol.* **140**, 59–68.
- SCHWIND, R. (1985). Sehen unter und über Wasser, Sehen von Wasser. *Naturwissenschaften* **72**, 343–352.
- STOCKTON, W. L. & COWEN, R. (1976). Stereoscopic vision in one eye: paleobiology of the schizochroal eye of trilobites. *Paleobiology* **2**, 304–315.
- TOWE, K. (1973). Trilobite eyes: calcified lenses *in vivo*. *Science* **179**, 1007–1010.
- WARRANT, E. J., MCINTYRE, P. D. & CAVENEY, S. (1990). Maturation of optics and resolution in adult dung beetle superposition eyes. *J. Comp. Physiol. A* **167**, 817–825.
- WATERMAN, T. H. (1981). Polarization sensitivity. In: *Comparative Physiology and Evolution in Invertebrates. B: Invertebrate Visual Centers and Behavior I. Handbook of Sensory Physiology VII/6B*. (Autrum, H., ed.) pp. 281–469. Berlin: Springer Verlag.
- YAMASHITA, S. & TATEDA, H. (1976). Spectral sensitivities of jumping spider eyes. *J. Comp. Physiol.* **105**, 29–41.
- ZHANG, X. G. & CLARKSON, E. N. K. (1990). The eyes of lower Cambrian eodiscid trilobites. *Palaeontol. oggy* **33**, 911–932.